Available online at www.eccomasproceedia.org
Eccomas Proceedia COMPDYN (2023) 2062-2069

ECCOMAS
Proceedia

COMPDYN 2023
9th ECCOMAS Thematic Conference on
Computational Methods in Structural Dynamics and Earthquake Engineering
M. Papadrakakis, M. Fragiadakis (eds.)
Athens, Greece, 12-14 June 2023

SIMULATION OF THE HYSTERETIC BEHAVIOR OF TIMBER CONNECTIONS BY THE VAIANA-ROSATI MODEL: PRELIMINARY RESULTS

A. Spedicato, N. Vaiana and L. Rosati

Department of Structures for Engineering and Architecture, University of Naples Federico II
via Claudio 21, 80125 Naples, Italy
e-mail: agnese.spedicato@unina.it

Abstract. *This paper illustrates the simulation of the complex hysteresis loops obtained by a cyclic experimental test carried out on an angular bracket; the related experimental data have been retrieved from the current scientific literature. In particular, the pinched and asymmetric hysteresis loop shapes are reproduced by using the recently formulated Vaiana-Rosati (VR) model of hysteresis. The preliminary results shown in this work suggest that such a model can easily simulate the typical complex experimental responses generally exhibited by timber connections.*

Keywords: hysteresis loop, timber connection, Vaiana-Rosati model.

ISSN:2623-3347
Peer-review under responsibility of the organizing committee of COMPDYN 2023.
doi: 10.7712/120123.10542.21131

1 INTRODUCTION

Timber structures are spreading all over the world thanks to the numerous technical advantages that the use of wood offers. In particular, it allows for ease of assembly on site, high lightness and strength in relation to weight. In addition, it meets the demand for sustainability in construction it compared to the traditional materials, such as steel or concrete, that require a great deal of energy to build and consume just as much during their life cycle.

Furthermore, timber structures show effective resistance to seismic loads, even though the general behavior of these structures is brittle. The use of metal joints allows it to properly react to a dynamic input, relatively to its degree of ductility, exhibiting complex force-displacement hysteresis loops that are indicative of the dissipation of energy during history loading and of the deformations achieved by the structure without collapsing.

Considering the low capacity of timber to tolerate cyclic loads, the specific hysteresis loops of timber structures are assimilated to those of the single connections. Therefore, there are different loop shapes, depending upon the typology of connection [1, 2], with one or two share planes or with single fasteners or plates, hold-down and angle brackets. Accordingly, the hysteresis loop shapes of timber connections are much more complex than those defining other materials. Specifically, the typical hysteresis loop shapes are affected by two different phenomena: pinching as well as force and/or stiffness deterioration. In this way the area enclosed by a given cycle tends to reduce for each loop, what produces a decrease in energy dissipation and strength resistance.

As a matter of fact, knowledge of the actual structural behavior of timber systems during seismic events is lacking. Also in the current Design Codes, there are parameters, such as the behavior factor, that approximate the capacity of dissipation energy, without a strict link with the design of steel connections.

In the scientific literature, researchers have developed several phenomenological models to predict the behavior of timber connections [3]. Unfortunately, the existing models appear to be rather to be implemented in a computer code; furthermore, the physical meaning of the adopted parameters is not always very clear. For these reasons, in this paper, we adopt a model recently formulated by Vaiana and Rosati [4], i.e. a new phenomenological hysteresis model capable of simulating different types of complex hysteresis loops adopting parameters having a clear mechanical meaning. Furthermore, the VR model turns out to be accurate, computationally efficient and easy to be implemented in a computer program.

2 TYPICAL TIMBER CONNECTION HYSTERESIS LOOPS

The timber connection taken into consideration in this paper is an angular bracket tested by Gavric et al. [5] within the SOFIE project [6]. The type of connection used is the BMF (*Board Measured Foot*) 90x116x48x3mm with 11 annular ringed nails 4x60 mm, see, e.g., Figure 1. Monotonic and cyclic tests were carried out on a CLT panel with 5 orthogonally crossed layers, each one ticked 17 mm. The cyclic test was carried out using a velocity input ranging from 0.4 mm/s to 0.8 mm/s. The tested specimen exhibited a good behavior in shear and good ductility up to 30 mm. Failure of the connection occurred when the steel nails reached the yielding point with the formation of two plastic hinges and a slight ovalisation of the hole around the nail.

The hysteretic loop derived from the experimental test is affected by a significant pinching phenomenon and stiffness degradation, caused by the progressive slipping of the nails. As shown in Figure 3a, for each loop there is a slight degradation of the strength relating to the progressive decrease of the capability to dissipate energy.

(a)  (b) 

Figure 1: (a) Specimen set-up of an angle bracket connected to a CLT panel loaded in shear and (b) angle bracket near the collapse during the cyclic test. [5]

3 VAIANA-ROSATI MODEL

The experimental hysteresis loops deriving from the tests performed on the above-described angle bracket are simulated using the Vaiana-Rosati Model (VRM) recently published in [4]. This model descends from an existing class of uniaxial phenomenological models [7, 8, 9, 10, 11] and can simulate the complex hysteresis loops of many materials and mechanical systems. Moreover, it permits the evaluation of the generalized force in closed form, considerably reducing the effort in computation. For the sake of completeness, the VRM is briefly summarized in this section.

In the formulation of the VRM, the generalized force f (generalized displacement u) represents the output (input) variable of the generalized force-displacement hysteresis loop. It is characterized by two different phases: the generic loading and unloading phases. During the first one the velocity is positive ($\dot{u} > 0$) and the expression of the generalized hysteretic force f_{ri} turns out to be:

$$f_{ri}\left(u, u_j^+\right) = \begin{cases} c^+\left(u, u_j^+\right) & \text{when} \quad u < u_j^+ \quad \text{(1a)} \\ c_u\left(u\right) & \text{when} \quad u > u_j^+. \quad \text{(1b)} \end{cases}$$

Alternatively, during the second one, the velocity is negative ($\dot{u} < 0$) and the generalized hysteretic force f_{ri} becomes:

$$f_{ri}\left(u, u_j^-\right) = \begin{cases} c^-\left(u, u_j^-\right) & \text{when} \quad u > u_j^- \quad \text{(2a)} \\ c_l\left(u\right) & \text{when} \quad u < u_j^-. \quad \text{(2b)} \end{cases}$$

In particular, the generic loading phase is described by the generic loading curve c^+ and the upper limiting curve c_u. They have the following expressions:

$$\begin{aligned} c^+(u, u_j^+) = \beta_1^+ e^{\beta_2^+ u} - \beta_1^+ + \frac{4\gamma_1^+}{1 + e^{-\gamma_2^+\left(u - \gamma_3^+\right)}} - 2\gamma_1^+ \\ + k_b^+ u + f_0^+ - \frac{1}{\alpha^+}\left[e^{-\alpha^+\left(+u - u_j^+ + \bar{u}^+\right)} - e^{-\alpha^+ \bar{u}^+}\right], \end{aligned} \tag{3}$$

$$c_u(u) = \beta_1^+ e^{\beta_2^+ u} - \beta_1^+ + \frac{4\gamma_1^+}{1 + e^{-\gamma_2^+(u-\gamma_3^+)}} - 2\gamma_1^+ + k_b^+ u + f_0^+, \tag{4}$$

On the other hand, the generic unloading phase is described by the generic unloading curve c^- and the lower limiting curve c_l, with the following expressions:

$$\begin{aligned} c^-(u, u_j^-) = {} & \beta_1^- e^{\beta_2^- u} - \beta_1^- + \frac{4\gamma_1^-}{1 + e^{-\gamma_2^-(u-\gamma_3^-)}} - 2\gamma_1^- \\ & + k_b^- u - f_0^- + \frac{1}{\alpha^-}\left[e^{-\alpha^-\left(-u+u_j^-+\bar{u}^-\right)} - e^{-\alpha^-\bar{u}^-}\right], \end{aligned} \tag{5}$$

$$c_l(u) = \beta_1^- e^{\beta_2^- u} - \beta_1^- + \frac{4\gamma_1^-}{1 + e^{-\gamma_2^-(u-\gamma_3^-)}} - 2\gamma_1^- + k_b^- u - f_0^-. \tag{6}$$

The parameters u_j^+ and u_j^- represent the internal variables of the generic hysteresis loop and are computed as:

$$\begin{aligned} u_j^+ = {} & u_P + \bar{u}^+ + \frac{1}{\alpha^+}\ln\left\{+\alpha^+\left[\beta_1^+ e^{\beta_2^+ u_P} - \beta_1^+ + \frac{4\gamma_1^+}{1 + e^{-\gamma_2^+(u_P-\gamma_3^+)}} - 2\gamma_1^+\right.\right. \\ & \left.\left. + k_b^+ u_P + f_0^+ + \frac{1}{\alpha^+}e^{-\alpha^+\bar{u}^+} - f_P\right]\right\}, \end{aligned} \tag{7}$$

$$\begin{aligned} u_j^- = {} & u_P - \bar{u}^- - \frac{1}{\alpha^-}\ln\left\{-\alpha^-\left[\beta_1^- e^{\beta_2^- u_P} - \beta_1^- + \frac{4\gamma_1^-}{1 + e^{-\gamma_2^-(u_P-\gamma_3^-)}} - 2\gamma_1^-\right.\right. \\ & \left.\left. + k_b^- u_P - f_0^- - \frac{1}{\alpha^-}e^{-\alpha^-\bar{u}^-} - f_P\right]\right\}, \end{aligned} \tag{8}$$

in which, u_P and f_P depend on the position of the generic point P taken from the curve c^+ or c^-. Moreover, k_b^+, f_0^+, α^+, β_1^+, β_2^+, γ_1^+, γ_2^+, γ_3^+ (k_b^-, f_0^-, α^-, β_1^-, β_2^-, γ_1^-, γ_2^-, γ_3^-) represent the eight model parameters to be identified by using experimental or numerical tests results, specific for the loading (unloading) phase.

Finally, $\bar{u}^+$ and $\bar{u}^-$ constitute the internal model parameters that can be evaluated, respectively, as functions of α^+ and α^-:

$$\bar{u}^+ = -\frac{1}{\alpha^+}\ln(\delta_k^+), \tag{9}$$

$$\bar{u}^- = -\frac{1}{\alpha^-}\ln(\delta_k^-). \tag{10}$$

where $\delta_k = 10^{-20}$ is established on the basis of numerical experiments.

4 SIMULATION OF THE EXPERIMENTAL HYSTERESIS LOOPS

The performance of the Vaiana-Rosati model is proved by reproducing the experimental test carried out on the angular bracket introduced in Section 2. The related complex hysteresis loops are illustrated in Figure 3a.

Figure 2 shows the time history of the sinusoidal displacement adopted as input variable in both the experimental and numerical tests. It is characterized by an increasing value of the amplitude a, ranging from 3.6 mm to 32 mm, and by a time duration of 9.5 s.

In this preliminary work, to easily identify the model parameters, the entire experimental response is decomposed in a set of loading and unloading curves. As shown in Figure 3a, they are respectively identified by using the letters of their initial and final points. As an example, curve AB represents the loading curve connecting point A with point B.

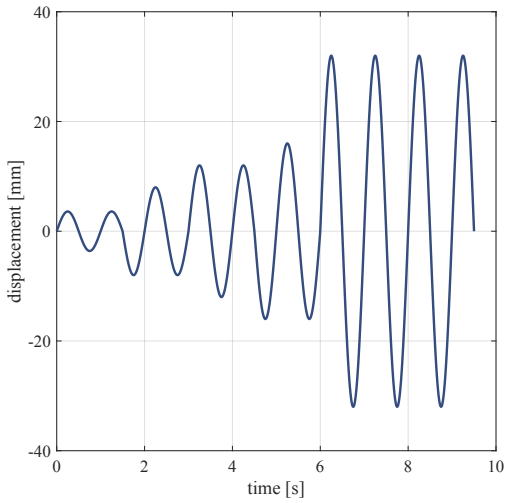

Figure 2: Applied harmonic displacement.

Actually, we shall note that the proposed model allows one to calibrate the parameters governing the loading phase separately from those ruling the unloading one. Consequently, it is possible to simulate very complex hysteresis loop shapes, as those affected by significant phenomena of pinching and stiffness degradation.

Table 1 presents the model parameters identified for each curve of the experimental response illustrated in Figure 3a.

Finally, Figure 3b compares the experimental hysteresis loops with those simulated by using the proposed model. Such a comparison reveals a good match between them and shows the potentiality of the VRM to reproduce very complex hysteretic responses.

5 CONCLUSIONS

This paper addresses the simulation of the experimental behavior characterizing a timber joint by utilizing the Vaiana-Rosati model.

The calibration of the parameters is performed by hand for each curve defining the experimental response. Despite its simplicity, the calibration approach allows for an accurate simulation of the complex experimental hysteresis loops.

In future work, we will propose analytical expressions to allow for the variation of the model parameters as functions of the work performed by the hysteretic force [12], as typically done in the literature [13]. In addition, an accurate identification procedure [14] will be adopted to drastically simplify the parameters calibration.

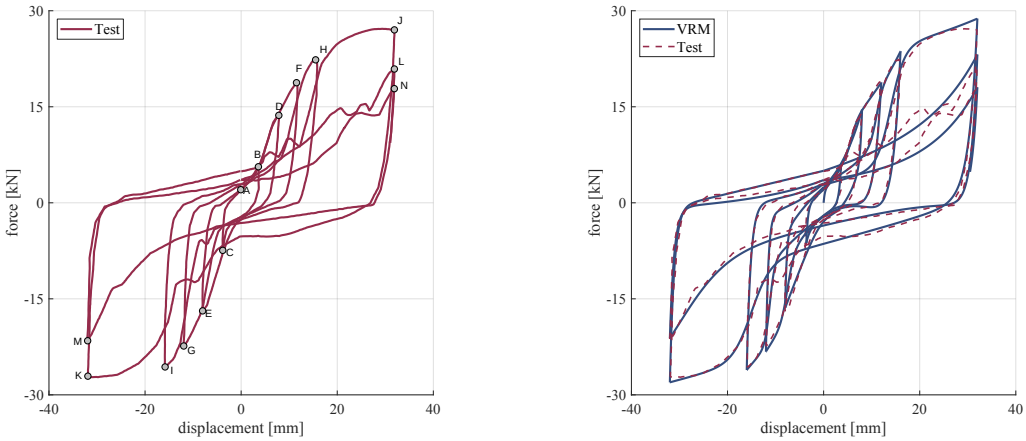

(a) (b)

Figure 3: (a) Experimental loops exhibited by an angular bracket with the indication of the initial and final points of each curve. (b) Simulation of the experimental loops by using the Vaiana-Rosati model.

curve	a	sign($\dot{u}$)	k_b	f_0	α	β_1	β_2	γ_1	γ_2	γ_3
	[mm]		[kN/mm]	[kN]	[1/mm]	[kN]	[1/mm]	[kN]	[1/mm]	[mm]
AB	3.6	+	0.7	2	4.1	0.11	0.65	0	0	0
BC		-	0.6	2.1	2.5	-0.015	-1.365	0	0	0
CD	8.0	+	1.1	2.35	2.5	0.5	0.3	1	-0.5	-0.5
DE		-	2.5	5.4	2.5	0	0.5	2.5	-0.6	1.8
EF	12.0	+	0.8	4.7	1.5	0.9	0.1	1.2	1.5	5.8
FG		-	1.25	7	0.6	-4.5	0.15	2.5	1.4	-7.5
GH	16.0	+	0.05	7	1.7	3	0.1	-2	-1.5	11
HI		-	1	8.3	0.6	-5.5	0.1	3.1	2	-11.2
IJ	32.0	+	0.2	12	1.1	0.05	0.1	4.6	0.7	14
JK		-	0.2	14	0.6	0.05	0.1	3.8	0.5	-15
KL		+	0.2	5	1	0.5	0.1	0	0	0
LM		-	0.18	13.5	0.8	-0.1	0.11	5	0.2	-30
MN		+	0.05	8	1.1	0.28	0.1	3.5	0.1	15

Table 1: Model parameters used to reproduce the experimental hysteresis loops of the tested angular bracket.

REFERENCES

[1] A. Awaludin, T. Hirai, Y. Sasaki, T. Hayashikawa, A. Oikawa, *Beam to column timber joints with pretensioned bolts*, Civil Engineering Dimension, **13**(2): 59-64, 2011.

[2] J.Q. Yang, S.T. Smith, Z. Wang, P. Feng, N. Sirach, *Modelling of hysteresis behaviour of moment-resisting timber joints strengthened with FRP composites*, International Journal of Mechanical Sciences, **179**: 105593, 2020.

[3] H. Dong, M. He, X. Wang, C. Christopoulos, Z. Li, Z. Shu, *Development of a uniaxial hysteretic model for dowel-type timber joints in OpenSees*, Construction and Building Materials, **288**: 123112, 2021.

[4] N. Vaiana and L. Rosati, *Classification and unified phenomenological modeling of complex uniaxial rate-independent hysteretic responses*, Mechanical Systems and Signal Processing, **182**: 109539, 2023.

[5] I. Gavric, A. Ceccotti, M. Fragiacomo, *Experimental cyclic tests on cross-laminated timber panels and typical connections*, na, 2011.

[6] P. Shiling et al. *Cross-laminated timber for seismic regions: Progress and challenges for research and implementation*, Journal of Structural Engineering, **142**(4): E2514001, 2016.

[7] N. Vaiana, S. Sessa, F. Marmo, L. Rosati, *A class of uniaxial phenomenological models for simulating hysteretic phenomena in rate-independent mechanical systems and materials*, Nonlinear Dynamics, **93**: 1647–1669, 2018.

[8] N. Vaiana, S. Sessa, F.Marmo, L. Rosati, *Nonlinear dynamic analysis of hysteretic mechanical systems by combining a novel rate-independent model and an explicit time integration method*, Nonlinear Dynamics, **98**: 2879–2901, 2019.

[9] N. Vaiana, S. Sessa, F.Marmo, L. Rosati, *An accurate and computationally efficient uniaxial phenomenological model for steel and fiber reinforced elastomeric bearings*, Composite Structures, **211**: 196–212, 2019.

[10] N. Vaiana, S. Sessa, L. Rosati, *A generalized class of uniaxial rate-independent models for simulating asymmetric mechanical hysteresis phenomena*, Mechanical Systems and Signal Processing, **146**: 106984, 2021.

[11] N. Vaiana, R. Capuano, S. Sessa, F. Marmo, L. Rosati, *Nonlinear dynamic analysis of seismically base-isolated structures by a novel opensees hysteretic material model*, Applied Sciences, **11**(3): 900, 2021.

[12] N. Vaiana, R. Capuano, L. Rosati, *Evaluation of path-dependent work and internal energy change for hysteretic mechanical systems*, Mechanical Systems and Signal Processing, **186**: 109862, 2023.

[13] R. Capuano, N. Vaiana, D. Pellecchia, L. Rosati, *A Solution Algorithm for a Modified Bouc-Wen Model Capable of Simulating Cyclic Softening and Pinching Phenomena*, IFAC-PapersOnLine, **55**(20): 319–324, 2022.

[14] S. Sessa, N. Vaiana, M. Paradiso, L. Rosati, *An inverse identification strategy for the mechanical parameters of a phenomenological hysteretic constitutive model*, Mechanical Systems and Signal Processing, **139**: 106622, 2020.

[15] M. Latour and G. Rizzano, *Cyclic behavior and modeling of a dissipative connector for cross-laminated timber panel buildings*, Journal of Earthquake Engineering, **19**(1): 137–171, 2015.